Reply

Penning-trap–assisted study of ^{115}Ru beta decay

J. Rissanen[1,a], J. Kurpeta[2], A. Płochocki[2], V.-V. Elomaa[1,b], T. Eronen[1], J. Hakala[1], A. Jokinen[1], A. Kankainen[1],
P. Karvonen[1], I.D. Moore[1], H. Penttilä[1], S. Rahaman[1,c], A. Saastamoinen[1], W. Urban[2,3], C. Weber[1,d], and J. Äystö[1]

[1] Department of Physics, P.O.B. 35, FIN-40014, University of Jyväskylä, Finland
[2] Faculty of Physics, University of Warsaw, ul. Hoża 69, 00-681 Warsaw, Poland
[3] Institut Laue-Langevin, 6 rue J. Horowitz, F-38042 Grenoble, France

Abstract. The beta decay of ^{115}Ru has been studied by means of Penning-trap–assisted beta and gamma spectroscopy at the IGISOL facility. The level scheme of ^{115}Rh has been substantially extended and compared with the level systematics of lighter rhodium isotopes. Tentative candidates for three states of the deformed $K = 1/2$ band have been suggested. The beta-strength distribution of the beta decay of ^{115}Ru differs from the beta decays of ^{111,113,113m}Ru isotopes due to non-observation of the 3-quasiparticle states in ^{115}Rh. The decay properties of ^{115}Ru indicate a spin-parity of $(3/2^+)$ for its beta-decaying ground state. In addition, possible Nilsson states as well as the shape and spin transitions in odd neutron-rich ruthenium isotopes are discussed.

1 Introduction

Neutron-rich ruthenium and rhodium isotopes around $A \sim 110$ are located in the region of changing nuclear shapes and shape coexistence between the strongly deformed zirconium and spherical tin isotopes. The structure studies of these nuclei are of importance for the astrophysical rapid neutron capture process (r-process) network calculations. Since the r-process nuclei are not yet experimentally accessible in this region, information about the lighter nuclei may help to predict the properties of more neutron-rich nuclei.

On the neutron-rich side of the nuclide chart, the ruthenium isotopes are considered to undergo two shape transitions. The first transition is from spherical vibrators to triaxial γ-soft nuclei (around $A \sim 104$–110) [1–6], with increasing rigidity when going towards more neutron-rich species [6–9]. The exact location of the second shape transition, from triaxial prolate to triaxial oblate [10], is diffi-

cult to predict due to its sensitivity to the model assumptions. For example, it has been predicted to take place at $A = 108$ [11] or at $A = 110$ [12,13]. Recently, experimental high-spin data [14,15], supported by theoretical results, suggest the transition to take place at ^{111}Ru [14–16].

The odd-proton ($Z = 45$) rhodium isotopes are located at the deformed proton mid-shell, 5 protons below the major $Z = 50$ shell closure. Spectroscopic studies of the rhodium isotopes are usually motivated by the presence of $v = 3$ seniority and the identification of a prolate $K = 1/2$ intruder band at low energy, originating from the down-sloping $1/2^+[431]$ proton orbital, crossing the $Z = 50$ shell gap and intruding among the spherical configurations built on the $g_{9/2}$ and $p_{1/2}$ subshells. The existence of the low-lying $K = 1/2$ intruder band and the hindered transitions out from that band have been taken as evidence of shape coexistence in rhodium isotopes. In addition to the prolate intruder band, a spherical ground state and excited states have been proposed to coexist. In refs. [17–19] a different conclusion has been suggested, in which the ground state and the first excited states in $^{107-113}$Rh isotopes are not spherical, but have triaxial prolate deformation. In this interpretation the large retardations of the decays out of the $K = 1/2$ band are not due to different shapes but K-hindrance.

The ^{115}Ru isotope is the most neutron-rich nucleus of the ruthenium isotopic chain presently available as a monoisotopic beam for spectroscopy studies at the JYFL-TRAP facility, Jyväskylä. It was discovered by Äystö *et*

[a] e-mail: juho.j-a.rissanen@jyu.fi
[b] *Present address:* Turku PET Centre, Accelerator Laboratory, Åbo Akademi University, FI-20500 Turku, Finland.
[c] *Present address:* Physics Division, P-23, Mail Stop H803, Los Alamos National Laboratory, Los Alamos, NM 87545, USA.
[d] *Present address:* Fakultät für Physik, Ludwig-Maximilians-Universität München, Am Coulombwall 1, D-85748 Garching, Germany.

al. [20], via a 293 keV gamma transition in ^{115}Rh belonging to the beta decay of ^{115}Ru. The beta decay of ^{115}Ru has been studied in three different experiments at the IGISOL facility. Based on the first test experiment, which took place in 2006, the first level scheme of ^{115}Rh was published [21]. A slightly extended level scheme of ^{115}Rh based on the second experiment in 2008 was published in a conference proceedings [22] and the partial decay scheme of ^{115}Rh in ref. [23]. The third experiment was performed in February 2010, and it was dedicated to the half-life measurement of ^{115}Ru, see ref. [24]. In this paper, the preliminary beta-decay scheme of ^{115}Ru [21,22] is confirmed and extended to higher energies.

2 Experimental

Ruthenium ions were produced in light-ion–induced fission by bombarding a tilted, $15\,\mathrm{mg/cm^2}$ thick, natural uranium target with a 25 MeV proton beam from the K-130 cyclotron at the ion guide isotope separator on-line (IGISOL) facility [25,26]. Fission products recoiling out from the target were stopped and thermalized in collisions with helium gas atoms, transported out of the gas cell, guided through the sextupole ion guide (SPIG) [26] and accelerated to an energy of 30 keV. The reaction products with an average charge state of 1^+ were mass-separated with a $55°$ dipole magnet, which has enough resolving power ($\frac{M}{\Delta M} \sim 500$) to select the $A = 115$ isobars out of the reaction products. After deceleration and injection into a gas-filled radiofrequency quadrupole (RFQ) cooler-buncher [27], the bunched beam of ions were injected into the double Penning-trap setup, JYFLTRAP [28].

The JYFLTRAP setup consists of two cylindrical Penning traps housed in a warm bore of a 7 T superconducting solenoid. Only the first trap, the purification trap [28], was used in this study to select ^{115}Ru ions from the mass-separated $A = 115$ beam. The purification process was performed by a buffer-gas cooling technique [29]. In this technique, after thermalization of ions in collisions with buffer gas atoms, all ions are excited to larger radii by applying a radiofrequency radial electric dipole field with the magnetron frequency and then mass-selectively centering by applying a radiofrequency quadrupole electric field with the true cyclotron frequency of ^{115}Ru, $\nu_c = \frac{1}{2\pi}\frac{qB}{m} = 935190\,\mathrm{Hz}$. In extraction, only the centered ones can pass a diaphragm with a diameter of 2 mm. In the present experiment, the mass resolving power of the method was $\frac{M}{\Delta M} \approx 6 \cdot 10^4$, sufficient to prepare clean samples of ^{115}Ru ions.

The ^{115}Ru ions were transported through the second Penning trap and implanted into a movable tape surrounded by the detector setup located after the Penning traps. The detector setup consists of a 2 mm thick plastic scintillation detector and three Ge detectors to measure the β- and γ-radiation, respectively. A planar Ge detector (LOAX) with a thin Be window was used for collection of X-rays and low-energy γ-rays, whereas two coaxial HPGe detectors measured the γ-radiation up to 4 MeV.
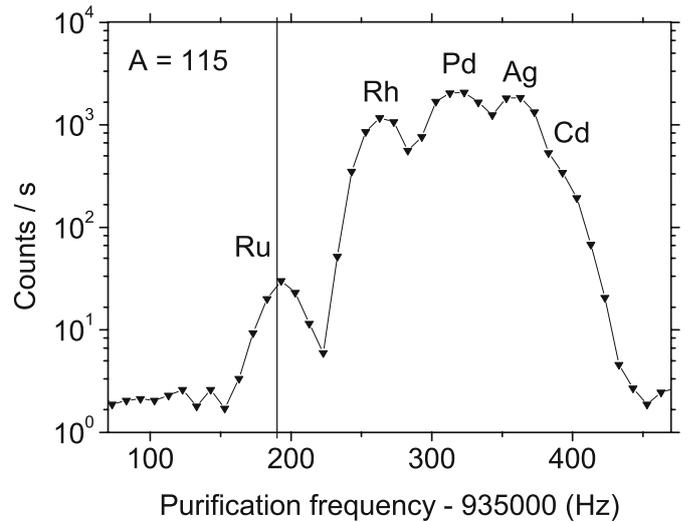
Fig. 1. Ion counts registered with the MCP detector located after the Penning trap as a function of the purification frequency. The trap settings were optimized to maximize the transmission of the ^{115}Ru ions.

The detector setup was calibrated with standard calibration sources.

The trap was operated in cycles of 111 ms. After every cycle one bunch of ^{115}Ru ions was implanted into the tape. The cycle consisted of a 40 ms cooling time period followed by 10 ms of magnetron excitation and 40 ms of cyclotron excitation. Before the extraction, an additional 20 ms cooling time was used. After every 2700 trap cycles ($\approx 300\,\mathrm{s}$) the tape was moved to remove accumulated daughter activities. Such a long accumulation time was mainly due to problems in the tape transport system.
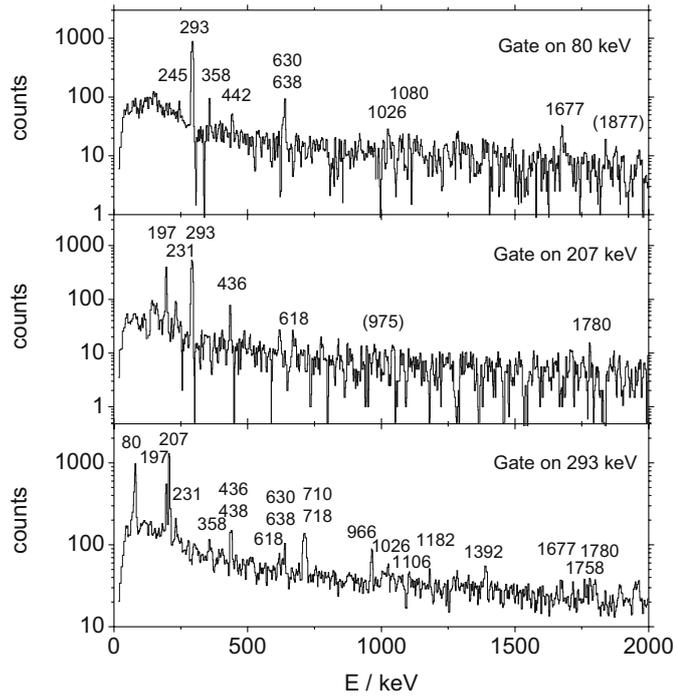
3 Results

The isobaric scan of mass 115, measured with the multi-channel-plate (MCP) detector located after the trap, is presented in fig. 1. One can notice how the ruthenium ions are clearly separated from the neighbouring isobars. The measured yield of ^{115}Ru was about 30 ions/s. Based on the isobaric scan, a proper purification frequency for ^{115}Ru was chosen. All beta-gated gamma rays observed in the detector setup could be assigned to the decay of ^{115}Ru or to the subsequent decay of its daughters. In this study we found altogether 34 gamma lines following the beta decay of ^{115}Ru. They are presented in table 1 with their intensities and coincidence relations. Coincidence spectra gated by the three most intense gamma lines are presented in fig. 2.

The β-γ coincidences were used to build a beta-decay scheme of ^{115}Ru, which is shown in fig. 3. Altogether 19 excited levels in ^{115}Rh have been found which are presented in table 2. When calculating the beta feedings and log ft values shown in table 2 the intensity values have been corrected with experimental or theoretical internal conversion coefficients from ref. [30], under the assumption of the

Table 1. Gamma transitions following the beta decay of ^{115}Ru. The notation ^{n} stands for a transition discovered in this work and ^{c} means that the transition has already been shown in a conference proceedings [22]. Weak transitions are in brackets. The relative gamma intensities have been taken from the β-gated singles spectrum except for the intensities for the triplet transitions (435.5-438.3-441.9 keV) and the low-intensity 239.2 keV, 974.9 keV and 1182.2 keV transitions, which have been taken from the β-γ coincidence spectra. The contribution of the 372.9 keV transition in ^{115}Ag has been subtracted from the intensity of the 372.5 keV transition.

E_γ (keV)	I_γ (%)	$E_i \rightarrow E_f$ (keV)	Coincident lines and remarks
80.1(2)	13.0(5)	$372.5 \rightarrow 292.5$	K_α(Rh), 245.1, 292.5, 358.4, 441.9, 630.0, 638.3, 1025.8, (1040.1), 1079.4, 1677.3, (1876.7), $I_{\gamma+e^-} = 24(5)$, ICC = 0.9(4), $M1$
$158.9(9)^n$	weak	$372.5 \rightarrow 213.2$	(213.2)
196.5(2)	10.3(5)	$696.0 \rightarrow 499.5$	K_α(Rh), 207.0, 239.2, 292.5
207.0(2)	30.6(10)	$499.5 \rightarrow 292.5$	K_α(Rh), 196.5, 231.4, 292.5, 435.5, 618.1, (974.9), 1780.6
$213.2(2)^n$	weak	$213.2 \rightarrow 0.0$	(158.9), (404.2)
$231.4(2)^c$	2.3(8)	$730.9 \rightarrow 499.5$	K_α(Rh), 207.0, 292.5
$239.2(2)^n$	2.2(5)	$935.0 \rightarrow 696.0$	196.5, 207.0, (292.5)
$245.1(2)^n$	2.9(4)	$617.6 \rightarrow 372.5$	80.0, (292.5)
292.5(2)	100(4)	$292.5 \rightarrow 0.0$	K_α(Rh), 80.1, 231.4, 358.4, 435.5, 438.3, 441.9, 618.1, 638.3, 710.4, 718.3, 966.3, 1025.8, 1040.1, 1105.9, 1182.2, 1392.2, 1677.3, 1758,2, 1780.6
$358.4(2)^c$	2.9(6)	$730.9 \rightarrow 372.5$	80.1, 292.5, 372.5
372.5(2)	9.9(14)	$372.5 \rightarrow 0.0$	245.1, 358.4, 630.0, 638.0, 1025.8, 1079.4, (1677.3)
$404.2(6)^n$	weak	$617.6 \rightarrow 213.2$	(158.9), (404.2)
$435.5(2)^c$	3.8(5)	$935.0 \rightarrow 499.5$	207.0, 292.5
$438.3(2)^n$	3.2(23)	$730.9 \rightarrow 292.5$	K_α(Rh), 292.5
$441.9(2)^n$	4.6(10)	$1452.6 \rightarrow 1010.7$	80.1, 292.5, 638.3, 718.3
$618.1(2)^n$	1.8(2)	$1117.6 \rightarrow 499.5$	207.0, 292.5
$630.0(3)^n$	0.4(1)	$1002.6 \rightarrow 372.5$	80.1, 292.5, 372.5, 1246.8
$638.3(3)^c$	3.8(2)	$1010.7 \rightarrow 372.5$	K_α(Rh), 80.1, 292.5, 372.5, 441.9, 1040.1
$710.4(3)^n$	6.9(3)	$1002.6 \rightarrow 292.5$	292.5, (1246.8)
$718.3(3)^n$	3.7(2)	$1010.7 \rightarrow 292.5$	292.5, (441.9)
$966.3(3)^c$	2.4(3)	$1258.8 \rightarrow 292.5$	(K_α(Rh)), 292.5
$974.9(3)^n$	0.9(2)	$1474.7 \rightarrow 499.5$	(207.0), (292.5)
$1025.8(6)^n$	2.0(10)	$1398.3 \rightarrow 372.5$	80.1, 292.5, 372.5
$1040.1(4)^n$	2.8(6)	$2050.4 \rightarrow 1010.7$	80.1, 638.3
$1079.4(5)^n$	1.3(10)	$1002.6 \rightarrow 372.5$	(80.1), (292.5), (372.5)
$1105.9(9)^n$	0.9(5)	$1398.3 \rightarrow 292.5$	292.5
$1182.2(5)^n$	1.9(5)	$1474.7 \rightarrow 292.5$	292.5
$1246.8(9)^n$	1.7(4)	$2249.3 \rightarrow 1002.9$	292.5, (372.5), 630.0, 710.4
$1392.2(4)^n$	4.1(4)	$1684.7 \rightarrow 292.5$	292.5
$1677.3(5)^n$	2.5(3)	$2050.4 \rightarrow 372.5$	80.1, 292.5
$1758.2(12)^n$	1.3(4)	$2050.4 \rightarrow 292.5$	292.5
$1780.6(5)^n$	2.6(4)	$2280.1 \rightarrow 499.5$	207.0, 292.5
$1876.7(6)^n$	1.4(4)	$2249.3 \rightarrow 372.5$	80.1, 372.5
$2249.4(5)^n$	1.4(5)	$2249.3 \rightarrow 0.0$	

Fig. 2. Coincidence spectra gated by three different gamma lines in ^{115}Rh.

Table 2. Levels in ^{115}Rh fed by the β decay of ^{115}Ru. The notation ^{n} stands for a level discovered in this work and ^{c} means that the level has already been shown in a conference proceedings [22].

E_{level} (keV)	β feeding (%)	$\log ft$	I^π
0.0	–	–	$(7/2^+)$
$213.2(2)^n$	–	–	$(9/2^+)$
$292.5(2)$	15(6)	5.4(2)	$(3/2^+)$
$372.5(2)$	15(4)	5.4(2)	$(5/2^+)$
$499.5(2)$	9.4(13)	5.6(1)	$(3/2^+)$
$617.6(2)^n$	2.4(4)	6.2(1)	$(7/2^+)$
$696.0(2)^c$	7.4(6)	5.6(1)	$(3/2^+)$
$730.9(2)^n$	7(2)	5.7(2)	$(1/2^+)$
$935.0(2)^c$	5.0(6)	5.8(1)	$(5/2^+)$
$1002.9(3)^c$	4.6(2)	5.8(1)	
$1010.7(4)^c$	0.5(5)	6.7(5)	
$1117.6(3)^n$	1.5(2)	6.2(1)	
$1258.8(4)^c$	1.9(2)	6.1(1)	
$1398.3(7)^n$	2.4(10)	5.9(2)	
$1452.6(4)^n$	4.8(12)	5.6(2)	
$1474.7(5)^n$	2.3(5)	5.9(1)	
$1684.7(5)^n$	3.3(4)	5.7(1)	
$2050.4(4)^n$	5.4(6)	5.4(1)	
$2249.3(5)^n$	3.7(6)	5.5(1)	
$2280.1(6)^n$	2.1(3)	5.7(1)	

most probable multipolarity. The $Q_\beta = 8165(12)$ keV [31] and the $t_{1/2} = 318(19)$ ms [24] have been used in the $\log ft$ calculations. Due to a wide Q_β window of the ^{115}Ru beta decay and possible missing high-energy, low-intensity gamma transitions, the $\log ft$ values have to be considered as lower limits.

Since the implantation tape was moved only once in 300 s, the total beta feeding to states in ^{115}Rh is approximately equal to the total beta feeding to states in ^{115}Pd. Comparison of these two numbers, and assuming zero beta feeding to the ground state of ^{115}Pd, indicates that $6(6)\%$ of the total beta feeding going to the states in ^{115}Rh is not seen in this study. This feeding cannot go directly to the ground state due to a spin difference of 2 between the ground states of ^{115}Ru and ^{115}Rh. The feeding probably goes to various high-lying excited states, which de-excite to the ground state via unobserved low-intensity gamma transitions. Another option, a possibility that the isomer in ^{115}Ru [24] decays partly by beta decay cannot be completely ruled out, since it could explain the missing feeding and also a small feeding to the $(7/2^+)$ state at 617.6 keV. There has been no observation of beta-delayed neutron decay in this work. The decay scheme of ^{115}Rh is from ref. [32]

3.0.1 Internal conversion coefficient of the 80.1 keV transition

The K internal conversion coefficient $(\text{ICC}(K))$ for the 80.1 keV transition has been derived based on the fluorescence method [33], resulting in $\text{ICC}(K) = 0.9(4)$. In

the derivation, the multipolarity of the 292.5 keV transition was assumed to be $E2$. The theoretical value for an $M1$ transition, $\text{ICC}(K, M1) = 0.559(8)$ is within the experimental error bars. The theoretical value for an $E2$ transition is $\text{ICC}(K, E2) = 2.22(4)$, suggesting that some amount of mixing cannot be ruled out.

3.1 Spin and parity assignments of the levels

3.1.1 Ground state of ^{115}Ru

The strongest beta feedings were observed for the levels with spins of $(1/2^+ - 5/2^+)$. The spin-parity assignments of these levels will be discussed later in the text. The observed beta feedings favour a $(3/2^+)$ assignment for the ^{115}Ru ground state. In particular a reasonably strong beta feeding to the first $5/2^+$ state differs from the decay of the $1/2^+$ ground state of ^{113}Ru, in which no feeding to this level has been observed [34,35].

A $(1/2^+)$ assignment has been suggested in earlier publications [21,24] based on the analysis of the previous experiment at IGISOL. The data of the later experiments allow us to derive the beta feedings to the different levels more reliably and opens up the question of a new ground-state spin transition from $(1/2^+)$ at $A = 113$ to $(3/2^+)$ at $A = 115$. A similar spin transition has been suggested for palladium isotopes [23].

The $(1/2^+)$ assignment explains the lack of gamma transitions to the ^{115}Rh ground state and fits better to the level systematics of odd ruthenium $(Z = 44)$ isotopes, as presented in fig. 5 and in ref. [24], but with this assignment
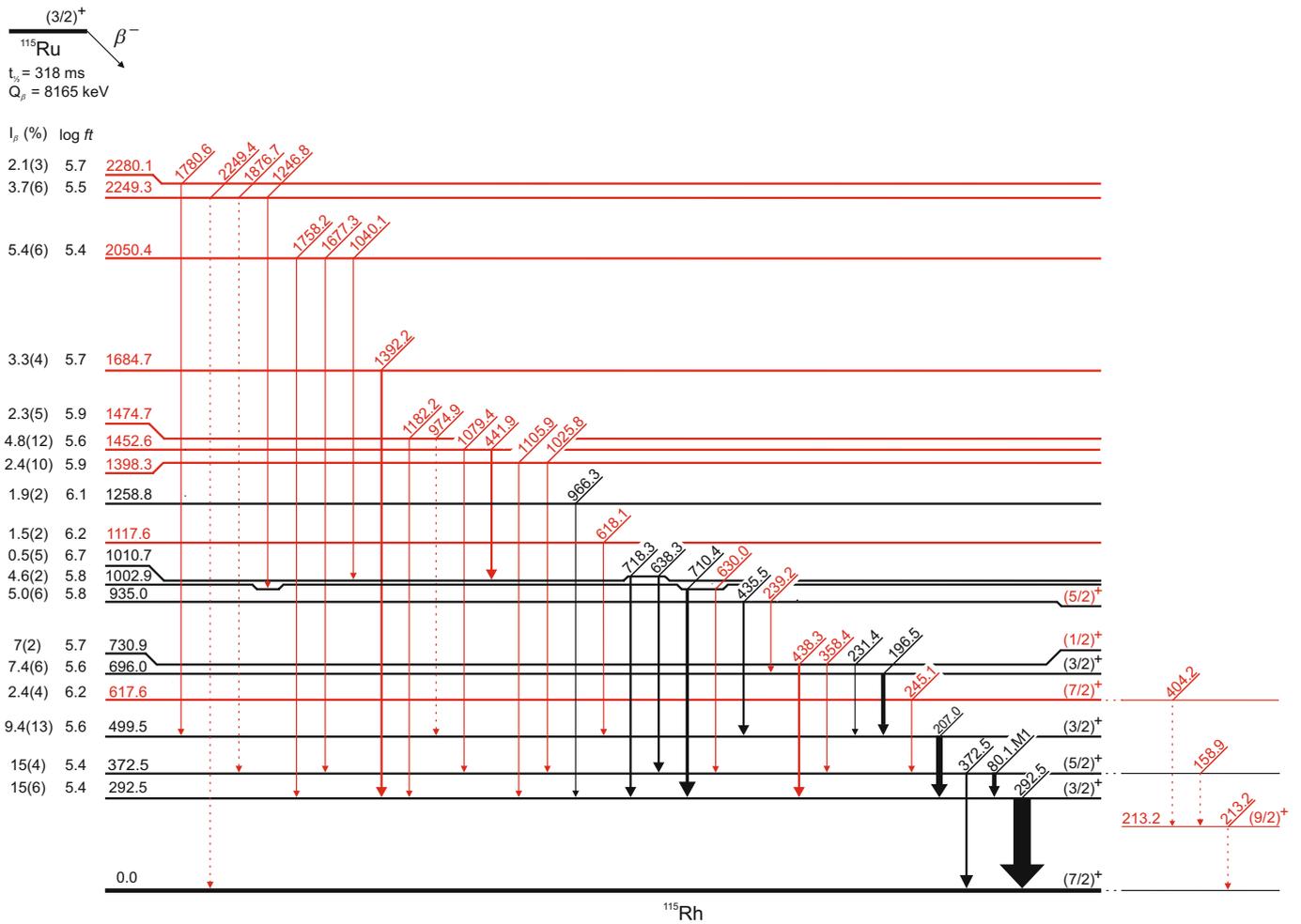
Fig. 3. (Colour online) Beta-decay scheme of ^{115}Ru. The levels and transitions drawn in red are new. Energies are in keV. The line widths correspond approximately to the transition intensities. The missing feeding of 6(6)% has not been placed in the decay scheme.

it is difficult to explain the strong beta feeding to the first $(5/2^+)$ state in ^{115}Rh. On the other hand, the $N = 71$ isotones ^{119}Cd [36] and ^{117}Pd [37], have ground-state spins of $3/2^+$. Since there is more experimental evidence and since it is supported by the level systematics of the $N = 71$ isotones, the $(3/2^+)$ assignment is preferred to previously reported $(1/2^+)$.

3.1.2 Ground state and excited states of ^{115}Rh

The ground state $(7/2)_1^+$. The spin and parity assignments of the ground state and three first excited states have been proposed already in an earlier study [21] based on the level systematics of lighter rhodium isotopes, see fig. 6. The $(7/2)^+$ is the only candidate for the spin assignment of the ground state based on systematics. The direct beta feeding is therefore strongly prohibited due to $\Delta I = 2$ character of this transition. Undetectable ground-state feeding has been pointed out in the lighter rhodium isotopes in refs. [34,38] also. Due to non-observation of the lowest-

intensity gamma transitions, 6(6)% of the beta feeding could not be placed in the decay scheme of fig. 3.

The tentative level at 213.2 keV $(9/2)_1^+$. A 213.2 keV transition is seen in the beta-gated singles spectrum. It is in weak coincidence with the 158.9 keV and 404.2 keV transitions, which are seen neither in the beta-gated singles spectrum nor in coincidence with other gamma transitions related to ^{115}Ru decay. A 212.8 keV gamma transition is found also in the decay of ^{115}Ag to ^{115}Cd. However, the ^{115}Rh peaks were more pronounced compared to the ^{115}Cd peaks, which were barely seen above the background in the coincidence spectrum gated by the 213 keV transition. Therefore, the 213.2 keV level is presented as a tentative level in the decay scheme to be confirmed by future measurements. The location of this level fits well to the level systematics, and a spin assignment of $(9/2)^+$ has been suggested. A coincidence spectrum gated on the 213.2 keV transition is presented in fig. 4

The level at 292.5 keV $(3/2)_1^+$. For the first excited state of ^{115}Rh, the most probable assignments are $(3/2)^+$ or $(9/2)^+$ based on systematics of the lighter rhodium isotopes. It is strongly fed by beta decay corresponding
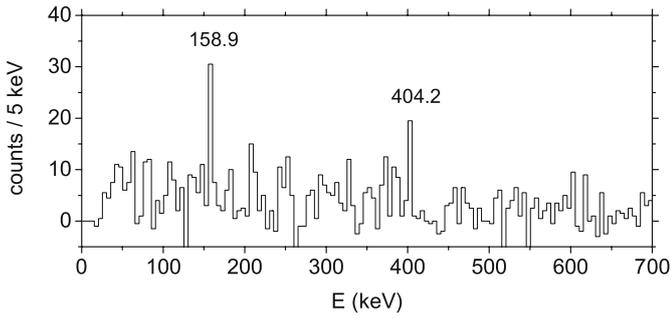
Fig. 4. A β-γ coincidence spectrum gated on the 213.2 keV transition.

to an allowed beta transition from the ground state of ^{115}Ru. Thus, a $(9/2)^+$ assignment can be ruled out. The strong beta feeding to the $(3/2)_1^+$ state indicates that the ground-state spin of ^{115}Ru has to be $I \leq 5/2$.

The level at 372.5 keV $(5/2)_1^+$. This level is connected to the $(3/2)_1^+$ level at 292.5 keV with a strong $M1$ transition and to the ground state with a weaker transition. A similar pattern has been observed in lighter rhodium isotopes. It has also relatively strong beta feeding, which implies $1/2^+ \leq I^\pi \leq 5/2^+$. The $(5/2)^+$ assignment can be chosen based on the level systematics. The beta-intensity ratio of $I_\beta(3/2)_1^+/I_\beta(5/2)_1^+ = 1.0(5)$ is close to the value of $I_\beta(3/2)_1^+/I_\beta(5/2)_1^+ \approx 1.6$ given by the Alaga rule for the rotational states [39], assuming $K = 3/2$ for the initial and final states. This suggests this level to be a member of the $K = 3/2$ band, with a $(3/2)_1^+$ band head and supports also the $(3/2^+)$ assignment for the ^{115}Ru ground-state spin. However, in the region of triaxiality, K is not a good quantum number and therefore the values given by the Alaga rule have to be taken only as a rough estimate.

The level at 499.5 keV $(3/2)_2^+$. This level is strongly fed by the beta decay of the ground state of ^{115}Ru with a $\log ft$ value of 5.6. This level has a strong connection to the first $(3/2)^+$ state and second $5/2^+$ state but no detectable connection to the ground state. These arguments suggest a low spin for the state. The $(3/2)^+$ assignment has been chosen although the $(1/2)^+$ could be also possible. Neither of these spin assignments fits in the level systematics of the lighter rhodium isotopes, which will be discussed later in more details. The 498.5 keV gamma transition from this level to the ground state, presented dashed in the decay scheme in ref. [22], has been left out from this paper. However, the $(3/2^+)$ assignment cannot explain the lack of a transition to the first $(5/2^+)$ state at 372.5 keV.

The level at 617.6 keV $(7/2)_2^+$. We can see only a weak transition to the first $(5/2)^+$ state at 372.5 keV. Level systematics of the lighter rhodium isotopes suggests this level to have spin of $7/2^+$, which is tentatively assigned here. This tentative assignment proposes that this level could be also the member of the possible $K = 3/2$ band. The lack of a transition to the $(3/2)^+$ state points against this argument but can be due to poor statistics. The next level of this band $9/2^+$ is not observed in our study. This level cannot be fed directly by the beta decay of the ^{115}Ru

ground state due to a $\Delta I = 2$ character of the possible beta transition. A feeding to this state shown in table 2 is due to either gamma cascades, which are too weak to be detected, or the gamma-decaying isomer in ^{115}Ru which decays also partly by beta emission.

The level at 696.0 keV $(3/2)_3^+$. This level is strongly fed by beta decay with an allowed character $(\log ft = 5.6)$, which limits possible spin assignments to $1/2^+ \leq I^\pi \leq 5/2^+$. It de-excites only to the low-spin state at 499.5 keV. The $(3/2)^+$ assignment was chosen based on the level systematics of the lighter rhodium isotopes. A possible interpretation for the structure of this level could be from the $K = 1/2$ intruder configuration, see the following discussion.

The level at 730.9 keV $(1/2)_1^+$. The beta-decay properties $(\log ft = 5.7)$ suggest $1/2^+ \leq I^\pi \leq 5/2^+$ for this level. It has connections to levels with spins of $(1/2^+)$ - $(5/2^+)$. The $(1/2)^+$ assignment was chosen based on systematics. The close-lying $1/2^+$ and $3/2^+$ states, with $3/2^+$ being lower in energy as well as the close-lying $5/2^+$ and $7/2^+$ states, with $7/2^+$ being lower in energy have been observed in lighter rhodium isotopes. This structure has been interpreted as a $1/2^+[431]$ intruder band originating above the $Z = 50$ shell gap having a strongly prolate-driving character. A simple extrapolation of the level systematics to $A = 115$ suggest the levels at 696.0 keV and 730.9 keV being the lowest members of that band. Estimates for the beta-branching ratios for these states given by the Alaga rule are $I_\beta(1/2)^+/I_\beta(3/2)^+ \approx 1.2$ for $K_i = I_i = 3/2, K_f = 1/2$ and $I_\beta(1/2)^+/I_\beta(3/2)^+ \approx 0.5$ for $K_i = I_i = 1/2, K_f = 1/2$. Both values are close to the measured value $I_\beta(1/2)^+/I_\beta(3/2)^+ = 1.0(3)$.

The level at 935.0 keV $(5/2)_2^+$. This level is fed by an allowed transition with a $\log ft$ value of 5.8 limiting the possible spin assignments to $1/2^+ \leq I^\pi \leq 5/2^+$. It de-excites to the levels at 696.0 keV and 499.5 keV with tentative spins of $(3/2)^+$. A spin assignment of $(5/2)^+$ is suggested based on the level systematics, which suggests also this level to be a member of the $K = 1/2$ intruder band. No connection to the $1/2^+$ state at 730.9 keV has been observed. The lack of the transition can be explained by the Alaga rule for the gamma transitions within a rotational band. The gamma-intensity ratio given by the Alaga rule is $I_\gamma(5/2^+ \rightarrow 3/2^+)/I_\gamma(5/2^+ \rightarrow 1/2^+) \approx 75$, which means that the $(5/2^+ \rightarrow 1/2^+)$ transition is beyond our detection limit.

4 Discussion

4.1 The ground state of ^{115}Ru

The ground-state spins of $1/2^+$ for ^{113}Ru and tentative $3/2^+$ for ^{115}Ru differ from the $5/2^+$ ground-state spin of lighter Ru isotopes, as shown in fig. 5. This spin transition can be related to the predicted shape transition [10] by inspecting the Nilsson diagram, see for example fig. 1 in ref. [10]. Assuming a reasonable prolate deformation $(\beta \approx 0.2)$ at $N = 65$ and $N = 67$, an unpaired neutron

Fig. 5. (Colour online) Level systematics of odd-mass neutron-rich ruthenium isotopes. The negative-parity levels are connected with dashed lines.

Table 3. Rotational constants in the $K = 1/2$ intruder band.

Nucleus	A (keV)	A_1 (keV)
^{111}Rh	19.6 [34]	−33.6 [34]
^{113}Rh	20.0 [34]	−26.8 [34]
^{115}Rh	18.1 (This work)	−29.6 (This work)

Fig. 6. (Colour online) Level systematics of odd-mass neutron-rich rhodium isotopes. The negative-parity states based on the $1/2^-[301]$ excitation are connected with dotted lines. The levels of the $1/2^+[431]$ intruder band are connected by dashed lines.

populates the $5/2[402]$ orbital originating from the $g_{7/2}$ spherical shell, as determined in ref. [40]. The $1/2[411]$ orbital, from the $s_{1/2}$ spherical shell, has been observed in neutron-rich isotopes around $A = 110$ [23]. This orbital can be populated in the ruthenium isotopic chain at $N = 69$, being on either the prolate or oblate side of the Nilsson diagram, and thus a possible configuration for the $1/2^+$ ground-state spin of ^{113}Ru. The $3/2[402]$ orbital from the $d_{3/2}$ spherical shell is close to the $1/2[411]$ orbital on the oblate side of the Nilsson diagram. Adding two more neutrons to ^{113}Ru$(N = 71)$ enables population of the $3/2[402]$ orbital, which could be a possible configuration for the ground state of ^{115}Ru. On the prolate side, the $3/2[402]$ orbital is not located near the Fermi level and therefore the $3/2^+$ ground-state spin of ^{115}Ru could be a possible sign of an oblate shape.

Gamow-Teller transitions in this region proceed via the transformation of a $g_{7/2}$ neutron into a $g_{9/2}$ proton. Therefore, it is possible that the ground state of ^{115}Ru has also components originating from the $g_{7/2}$ spherical state. Such states are for example $1/2[420]$ or $3/2[411]$.

4.2 K = 1/2 intruder band in rhodium

In lighter odd-A rhodium isotopes, the $K = 1/2$ intruder band originating from the $1/2^+[431]$ proton orbital above the $Z = 50$ major shell gap, has been identified [34,41]. Due to a large and negative decoupling parameter, there is an inversion of spins, the $3/2^+$ state being the band head instead of $1/2^+$. The same spin-inversion pattern remains up to higher spins [19]. The same $K = 1/2$ intruder band has been seen also in silver [42] and technetium isotopes [43]. To study the properties of this band in ^{115}Rh, we have used the notion of Bohr and Mottelson [44]:

$$E_I = E_0 + A\,I(I+1) + A_1(-1)^{I+1/2}(I+1/2)\delta(K, 1/2). \tag{1}$$

Since we have tentative candidates for three low-energy levels of this band, their energies can be used to calculate the coefficients A and A_1. The obtained values are compared to the values from the lighter rhodium isotopes in table 3. The calculated coefficients are similar for these three rhodium isotopes supporting the suggested spin assignments. However, this tentative interpretation needs to be confirmed by new experiments. For example, level lifetime measurements are required to address the question of shape coexistence and K-hindrance.

4.3 Level systematics of odd neutron-rich rhodium isotopes

The level systematics of the lighter odd-mass rhodium isotopes is presented in fig. 6. The tentative $(9/2)^+$ level fits well to the systematics. The beta feeding to this level is small or negligible, which indicates that the possible high-spin isomer in ^{115}Ru [24] is probably not a beta-decaying state as observed in ^{113}Ru [35].

The levels at 696.0 keV, 730.9 keV and 935.0 keV have been suggested to be members of the $K = 1/2$ intruder band, which is fitting well with the level systematics presented in fig. 6. The intruder levels exhibit a clear V shape with a minimum at $N = 64$ ($A = 109$) instead of $N = 66$ as already noted in refs. [41,42] indicating the maximal

Fig. 7. The beta-strength distributions of the ^{111,113,113m,115}Ru isotopes presented in the same scale. A strong peak around 2 MeV in ^{111,113,113m}Ru decays cannot be seen in the decay of ^{115}Ru. The data of ^{111,113,113m}Ru isotopes are from refs. [35,41].

deformation. The up-sloping trend seems to continue at $A = 115$.

Odd-parity levels in lighter rhodium isotopes are built on the $p_{1/2}$ shell ($1/2^-[301]$). The negative-parity levels are not fed by an allowed beta decay and they would be fed by first forbidden beta transitions, which have typically $\log ft$ values of around 6–9. The levels having a $\log ft$ value greater than 6 in an energy range suggested by systematics, are the 1010.7 keV, 1117.6 keV, and 1258.8 keV levels. However, none of these levels seem to be favorable candidates for this excitation and no levels have been assigned with negative parity.

Interpreting the 696.0 keV, 730.9 keV and 935.0 keV levels as $K = 1/2$ band members, introduces an "unexpected" low-spin state at 499.5 keV. The structure of this state remains unknown. Based on the de-excitations of this level and the 935.0 keV level, the spin-parities $1/2^-$ and $3/2^-$ could be possible for the 499.5 keV and 935.0 keV levels, respectively. However, these spin-assignments are not supported by the $\log ft$ values.

4.4 Beta-strength distribution

The beta-strength distributions of the decays of $^{111-115}$Ru have been calculated by using eq. (2) for the Gamow-Teller decay

$$B(GT) = \frac{1}{ft} \frac{C}{(\frac{G_A}{G_V})^2} , \qquad (2)$$

where $\frac{G_A}{G_V} = 1.2695(29)$ [45] is the ratio of the axial vector and vector coupling constants and $C = 6147.0(24)\,\mathrm{s}$ [46] is a constant. The beta-strength values are presented in fig. 7. The beta-strength distribution of ^{115}Ru decay differs from the distributions of the decays of ^{111,113,113m}Ru, whereby a remarkable part of the strength goes to the 3-quasiparticle states at around 2 MeV. In the case of ^{115}Ru the beta distribution is more equally distributed among different levels and no strong peaks are observed. This suggests a difference in the structures of either mother or daughter nuclei. In addition, the integrated value of 0.14 is smaller compared to the values of lighter rhodium isotopes, for example 0.27 for the ^{113}Ru decay and 0.35 for the ^{113m}Ru decay, calculated based on the $\log ft$ values from ref. [21]. Since there can be gamma transitions too weak to be detected, depopulating the levels above 2 MeV, the integrated value has to be interpreted as a lower limit.

The equal distribution of the beta strengths to several low-energy states has been suggested for oblate deformation in this region of the nuclide chart [47]. This means that studies of the beta-strength distribution offer a method to distinguish between prolate and oblate shapes [48]. However, for these studies, more theoretical and experimental work are needed to enable the comparison of the theoretical and experimental beta-strength values up to higher energies.

5 Conclusions

In this work the beta decay of the very neutron-rich ^{115}Ru has been studied by β- and γ-coincidence techniques. A monoisotopic source of ^{115}Ru was achieved by purifying the $A = 115$ beam from the IGISOL mass separator with the JYFLTRAP Penning-trap setup. The beta-decay scheme of ^{115}Ru has been extended. The level systematics of the rhodium isotopes has been extended to $A = 115$. Three candidates for the $K = 1/2$ intruder band members have been tentatively suggested, supported by calculated rotational constants. The existence of this band structure needs to be verified, for example, by high-resolution conversion electron spectroscopy [49] or level lifetime measurements [34,41].

The beta decay of ^{115}Ru differs from the decays of the lighter ruthenium isotopes since no strong beta feeding to the possible 3-quasiparticle states has been observed. The reasonably strong beta feedings to the low-spin states in ^{115}Rh let us postulate that the ^{115}Ru isotope has a low spin. The present data favors the $(3/2^+)$ assignment instead of the earlier announced $(1/2^+)$ [24]. The $(3/2^+)$ ground-state spin assignment changes also the spin of the

isomeric state from $(7/2^-)$ [24] to $(9/2^-)$ and the intermediate state from $(3/2^+)$ [24] to $(5/2^+)$.

Both ground-state spin assignments have candidate orbitals on the oblate side of the Nilsson diagram, which agree with the predicted prolate-oblate shape transition [10]. Due to the triaxial nature of the ruthenium isotopes, a gradual shape change is more probable instead of a rapid shape transition. Therefore, it is difficult to define the exact location of the shape transition either theoretically or experimentally. More experimental work, such as collinear laser spectroscopy measurements [50], in addition to new theoretical calculations are needed to answer to the questions of the ground state spin and deformation of ^{115}Ru.

References

1. J. Stachel, P. Van Isacker, K. Heyde, Phys. Rev. C **25**, 650 (1982).
2. J. Stachel *et al.*, Nucl. Phys. A **383**, 429 (1982).
3. J. Stachel *et al.*, Z. Phys. A **316**, 105 (1984).
4. J. Äystö *et al.*, Nucl. Phys. A **515**, 365 (1990).
5. J.C. Wang *et al.*, Phys. Rev. C **61**, 044308 (2000).
6. D. Troltenier *et al.*, Nucl. Phys. A **601**, 56 (1996).
7. Y. Luo *et al.*, Phys. Lett. B **670**, 307 (2009).
8. I. Stefanescu *et al.*, Nucl. Phys. A **789**, 125 (2007).
9. K. Zajac *et al.*, Nucl. Phys. A **653**, 71 (1999).
10. F.R. Xu, P.M. Walker, R. Wyss, Phys. Rev. C **65**, 021303 (2002).
11. G.A. Lalazissis, S. Raman, P. Ring, At. Data Nucl. Data Tables **71**, 1 (1999).
12. J. Skalski, S. Mizutori, W. Nazarewicz, Nucl. Phys. A **617**, 282 (1997).
13. P. Möller, J. Nix, W. Myers, W. Swiatecki, At. Data Nucl. Data Tables **59**, 185 (1995).
14. H. Hua *et al.*, Phys. Lett. B **562**, 201 (2003).
15. C.Y. Wu *et al.*, Phys. Rev. C **73**, 034312 (2006).
16. J.Q. Faisal *et al.*, Phys. Rev. C **82**, 014321 (2010).
17. Ts. Venkova *et al.*, Eur. Phys. J. A **6**, 405 (1999).
18. Ts. Venkova *et al.*, Eur. Phys. J. A **15**, 429 (2002).
19. Y.X. Luo *et al.*, Phys. Rev. C **69**, 024315 (2004).
20. J. Äystö *et al.*, Phys. Rev. Lett. **69**, 1167 (1992).
21. J. Kurpeta *et al.*, Eur. Phys. J. A **31**, 263 (2007).
22. J. Kurpeta *et al.*, Acta Phys. Pol. B **41**, 469 (2010).
23. J. Kurpeta *et al.*, Phys. Rev. C **82**, 027306 (2010).
24. J. Kurpeta *et al.*, Phys. Rev. C **82**, 064318 (2010).
25. J. Äystö, Nucl. Phys. A **693**, 477 (2001).
26. P. Karvonen *et al.*, Nucl. Instrum. Methods Phys. Res. B **266**, 4794 (2008).
27. A. Nieminen *et al.*, Nucl. Instrum. Methods Phys. Res. A **469**, 244 (2001).
28. V.S. Kolhinen *et al.*, Nucl. Instrum. Methods Phys. Res. A **528**, 776 (2004).
29. G. Savard *et al.*, Phys. Lett. A **158**, 247 (1991).
30. T. Kibédi *et al.*, Nucl. Instrum. Methods Phys. Res. A **589**, 202 (2008).
31. U. Hager *et al.*, Phys. Rev. C **75**, 064302 (2007).
32. J. Rissanen, Ph. D. Thesis, University of Jyväskylä, unpublished (2011).
33. J. Kantele, *Handbook of Nuclear Spectroscopy* (Academic press, London, 1995).
34. J. Kurpeta *et al.*, Eur. Phys. J. A **13**, 449 (2002).
35. J. Kurpeta *et al.*, Eur. Phys. J. A **33**, 307 (2007).
36. Y. Kawase, B. Fogelberg, J. McDonald, A. Bäcklin, Nucl. Phys. A **241**, 237 (1975).
37. D. Fong *et al.*, Phys. Rev. C **72**, 014315 (2005).
38. H. Penttilä, Ph. D. Thesis, University of Jyväskylä, JYFL Research Report No. 1/1992, unpublished (1992).
39. G. Alaga, K. Alder, A. Bohr, B. Mottelson, Dan. Mat. Fys. Medd. **29**, (1955).
40. C. Goodin *et al.*, Phys. Rev. C **80**, 014318 (2009).
41. G. Lhersonneau *et al.*, Eur. Phys. J. A **1**, 285 (1998).
42. J. Rogowski *et al.*, Z. Phys. A **337**, 233 (1990).
43. Y.X. Luo *et al.*, Phys. Rev. C **70**, 044310 (2004).
44. A. Bohr, B. Mottelson, *Nuclear structure*, vol. **2** (Benjamin, New York, 1975) p. 33.
45. W.-M. Yao *et al.*, J. Phys. G Nucl. Part. Phys. **33**, 1 (2006).
46. J.C. Hardy, I.S. Towner, Phys. Rev. C **71**, 055501 (2005).
47. P. Urkedal, X.Z. Zhang, I. Hamamoto, Phys. Rev. C **64**, 054304 (2001).
48. P. Sarriguren, J. Pereira, Phys. Rev. C **81**, 064314 (2010).
49. J. Rissanen *et al.*, Eur. Phys. J. A **34**, 113 (2007).
50. F. Charlwood *et al.*, Phys. Lett. B **674**, 23 (2009).